IEEE Access
Multidisciplinary | Rapid Review | Open Access Journal

Received May 8, 2019, accepted May 28, 2019, date of publication June 3, 2019, date of current version June 21, 2019.

Digital Object Identifier 10.1109/ACCESS.2019.2920523

Propagation Characteristics and Defect Sensitivity Analysis of Guided Wave From Single Excitation Source in Elbows

YU WANG, (Senior Member, IEEE), AND XUEYI LI
School of Mechanical Engineering, State Key Laboratory for Manufacturing and Systems Engineering, Xi'an Jiaotong University, Xi'an 710049, China
Corresponding author: Yu Wang (ywang95@xjtu.edu.cn)

This work was supported in part by the National Natural Science Foundation of China under Grant 61633001 and Grant 51875437, and in part by the China Postdoctoral Science Foundation under Grant 2014M560765 and Grant 2016T9090.

ABSTRACT Ultrasonic guided wave has received significant attention in the field of nondestructive testing because of their advantages in detecting the entire wall thickness. Since pipe elbows are an important component of the piping system, it is desirable to study the propagation behavior of the guided wave in the elbows. In this paper, instead of using the traditional method of a ring of transducers to generate guided wave at the same time, the propagation behavior of the guided wave in the elbows under the action of a single excitation source is simulated. Using the chirp excitation signal, the transmission signals of the guided wave at different excitation central frequencies are extracted with high efficiency, and the behavior of the guided wave in the elbow under different excitation frequencies is studied. In addition, it is proposed to use the flight time quantity to characterize the complete information of the structure, and the influence of the defects on the flight time is also studied. The results prove that the flight time feature has good detection sensitivity to the defects with varying depth in different locations of the elbow.

INDEX TERMS Single excitation source, S0 mode, flight time, detection sensitivity.

I. INTRODUCTION

Due to long propagation distance, fast detection speed, small attenuation and high efficiency, ultrasonic guided wave has gradually become an important direction for the research and development of pipeline nondestructive testing technology [1], [2].

In the decades of research that began with the analytical solution of the pipeline dispersion curve by Gazis [3], [4] in 1959, the propagation characteristics of the guided wave in the straight tube have made great progress [5]–[8] and the detection to defects such as cracks, notches and corrosion in straight hollow pipe have been studied by many researchers [9]–[13]. As an important component of the piping system, elbows are widely used in thermal power heat exchange tubes, oil and gas transportation pipelines [14] and has received lots of attention in recent years.

Unlike traditional ultrasonic inspections, due to the complexity of the elbow structure, the propagation of ultrasonic guided wave is more complicated. A number of studies on the propagation of the L(0,2) mode and T(0,1) mode as well as their reflection in bends have been carried out. Sanderson [15] studied the propagation characteristics of T(0,1) mode in the elbows and the amplitudes of the reflections can be significantly affected by the flaw via finite element method. Heinlein *et al.* [16] proved that the variation detection sensitivity of the torsional guided wave roughly follows the von Mises stress distribution for circumferential defects in bend. Zhang *et al.* [17] used low frequency excitation to emit guided wave to investigate the inspection of defects beyond elbows. Demma *et al.* [18] used finite element (FE) analysis to study the transmission and reflection coefficient of guided wave in a bend and indicated that the amplitude of reflected signal increases with the cross sectional area loss of the pipe caused by the defect [19]. A comprehensive study of the effects of bending angles on the transmission coefficient of T mode was reported in [20] by R. E. Jones using simulation and experimental methods. Nishino *et al.* [21] detected defects in circumferential welds before and after pipe bend using the T(0,1) mode ultrasonic guided wave and a wideband laser ultrasonic system was used to describe the propagation phenomena of wideband guided wave in bended pipes with

The associate editor coordinating the review of this manuscript and approving it for publication was Datong Liu.

2169-3536 © 2019 IEEE. Translations and content mining are permitted for academic research only.
Personal use is also permitted, but republication/redistribution requires IEEE permission.
See http://www.ieee.org/publications_standards/publications/rights/index.html for more information.

TABLE 1. Parameters of FE analysis.

Elastic modulus	Poisson ratio	Density	Unit type	Grid size	Number of Elements	Number of Nodes	computation time
210 GPa	0.3	7830 kg/m^3	Solid 164	2 mm	103616	192738	0.5 ms

time–frequency analysis [22]. Tan *et al.* [23] studied the defect detectability in pipes with elbows by using time delay focusing technique and common source method (CSM). Elbows with more general bend angles and a more general mean bend radius was considered by Verma *et al.* [24] to research the interaction of low–frequency axisymmetric ultrasonic guided wave with bends. It was found that the defect with different locations of the elbow can affect the reflection amplitude as well as the rates of mode conversion for T (0, 1) mode guided wave [25].

Previous studies have shown that the effect of elbow inspection is closely related to the location of defect distribution. Neither T(0,1) mode nor L(0,2) mode generated by a ring of transducers can-not accurately detect defects in intrados. What's more, the number of signal extracted from the monitoring points is limited to only one with the traditional excitation method, which in fact can-not provide sufficient information that reflect the structural integrity [26]. On the other hand, the entire circumference of the pipe is not completely accessible in many cases. Moreover, none of the previous studies has considered the relationship between the depth of defect in elbow and extracted signal characteristics which is an important characteristic when dealing with quantitative assessment of defects problem.

In order to solve the problems raised above, this paper studied the propagation characteristics of guided wave in elbows with a bend angle of 90° under the condition of single excitation source. The sensibility of flight time to defects with varying depth at specific areas of interest in elbows is also compared and discussed.

II. FINITE ELEMENT MODEL

A. CONSTRUCTION OF 3D FINITE ELEMENT MODEL

As discussed in Section I, numerical methods are effective and required for studying the scattering and propagation problems of ultrasonic guided wave. The ANSYS LS–DYNA module was used in this paper. Compared with the implicit finite element method, there is no convergence problem, and the solution time can be greatly shortened for a large number of meshes.

Geometrical characterization of the simulated elbow is shown in Fig. 1(a). Eight interested points are taken at both ends of the pipe as the signal excitation positions and signal monitoring positions respectively. For the convenience of later expression, the circumferential coordinates of the observation point are defined, wherein the points in extrados are 0° and the points in intrados are 180°. Additionally, circumferential crack–like defects with varying position

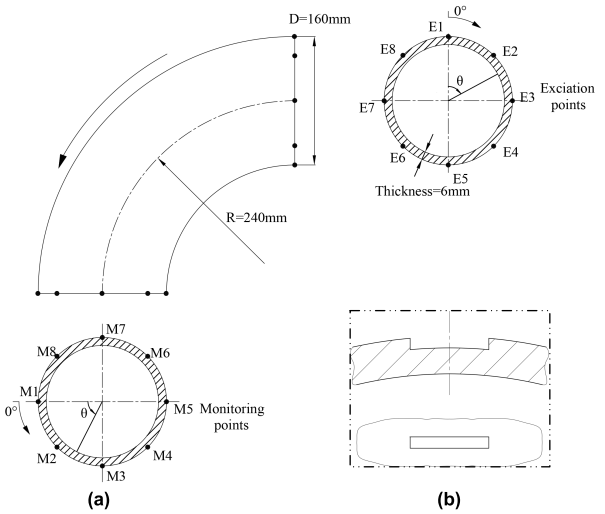

FIGURE 1. (a) Schematic of the elbow. Eight points for excitation and eight points for monitoring are chosen at both ends of the elbow. It needs to be stated that the excitation signal is applied at one of the eight excitation points (E1 to E8) each time. (b) Description of crack–like defects.

(intrados, extrados and middle of an elbow) and varying depth are simulated by removing the elements to evaluate defect sensibility of the extracted features. The width and length of defect in extrados is 2 mm, 6 mm respectively as Shown in Fig. 1(b).

Several parameters that should be determined before the analysis are shown in TABLE 1. Three elements were used through the thickness and the number of units in the thickness direction can ensure the accuracy of low frequency analysis [27]. The 3D finite element model is shown in Fig. 2.

B. EXCITATION SIGNALS

Chirp signal is a guided wave excitation signal optimization technique proposed by Michaels *et al.* [28]. The equation in time domain for chirp excitation is

$$s_c(t) = w(t)\sin\left(2\pi ft + \frac{\pi Bt^2}{T}\right) \tag{1}$$

where $w(t)$ is rectangular window function, f is the starting frequency, T is the duration of the signal, and B is the bandwidth of chirp signal. The linear chirp signal in time domain was shown in Fig. 2(a) when set $f = 0$kHz, $B = 400$kHz and $T = 1$ms.

We can see from Fig. 3(b) and Fig. 3(c) is that the chirp signal has a wide excitation band, so that the excitation of the chirp signal can achieve equivalent effect as the tone burst

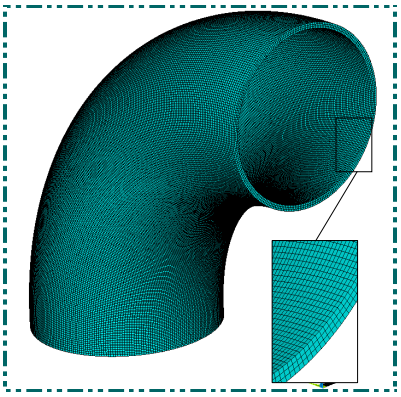

FIGURE 2. 3D finite element model. Three elements were used through the thickness.

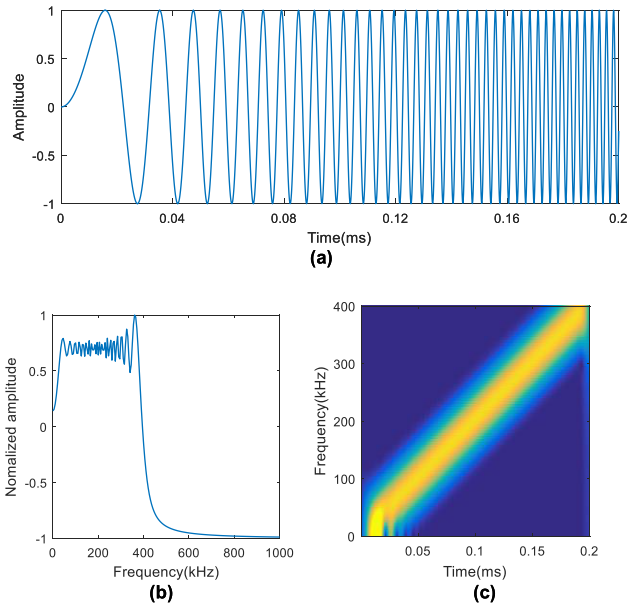

FIGURE 3. Chirp signal. (a) Time domain signal. (b) Frequency signal. (c) Time–frequency domain signal.

signal over the entire frequency band. In addition, the filtering process in chirp excitation can effectively improve the signal–to–noise ratio of the detection signal when extracting a large number of narrow–band responses.

In the frequency domain, the response signal to the chirp excitation can be written as

$$R_c(\omega) = H(\omega) S_c(\omega) \tag{2}$$

where $S_c(\omega)$ is the Fourier transform of $s_c(t)$. In a same guided wave detection system, $R_d(\omega)$ is the response to tone burst signal $S_d(\omega)$, and can be expressed as

$$R_d(\omega) = H(\omega) S_d(\omega) \tag{3}$$

By combining (2) and (3), the response to $S_d(\omega)$ are given as

$$R_d(\omega) = R_c(\omega) \frac{S_d(\omega)}{S_c(\omega)} \tag{4}$$

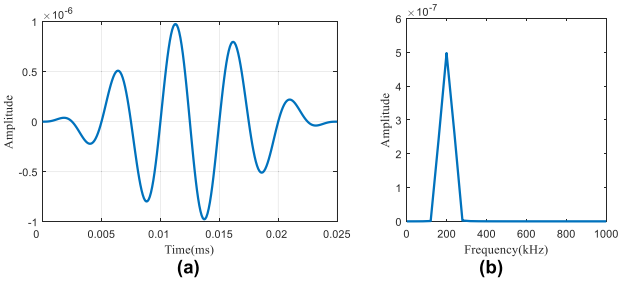

FIGURE 4. Tone burst modified by a Hanning window at 200 kHz central frequency. The issuance time of excitation signal at 200kHz is 0.0126 ms. (a) Time domain signal. (b) Frequency signal.

The desired excitation in this paper is the tone burst signal (Fig. 4), which is a Hanning windowed sinusoid with a duration of 5 cycles [29]. So the expression of $S_d(t)$ can be written as

$$s_d(t) = 0.5\left[(1 - \cos(\frac{2\pi f_c t}{5})\right] \sin(2\pi f_c t) \tag{5}$$

where f_c is the central frequency. So the response to tone burst signal can be extracted at varying central frequencies from 0 kHz to 400 kHz.

III. PROPAGATION CHARACTERISTICS ANALYSIS OF SINGLE EXCITATION SOURCE

Before the defect diagnosis, the analysis of the signal characteristics of the ultrasonic guided wave excited by single excitation source is an important step to determine the signal component and the central frequency to extract monitored signals.

Due to noise and other factors, the time–of–flight characteristics extracted from the measurements can be far more accurate than the amplitude characteristics in some cases. The short–time Fourier transform method is selected to convert the multi–modal ultrasonic guided wave signal into the time–frequency plane, which visually reflects the time–varying characteristics of each modal component.

In the time–frequency plane, the instantaneous frequency of the signal and the arrival time (t_a) of each frequency point correspond to the projection of the ridge line on the frequency and time axis, respectively [30]. Numerically, the flight time (t_f) of interested mode and the arrival time (t_a) following

$$t_f = t_a - t_e \tag{6}$$

where t_e is the issuance time of excitation signal at central frequency. The group velocities of the modes are then obtained as the ratio of the arc length (l_{arc}) at the elbow to the flight time, which can be expressed as

$$v = \frac{l_{arc}}{t_f} \tag{7}$$

The corresponding time traces for longitudinal chirp excitation of an elbow are shown in Fig. 5. Chirp response signal was extracted according to the signal extraction process

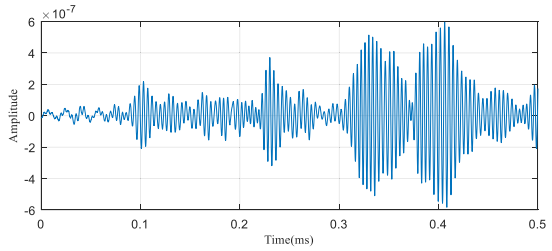

FIGURE 5. Response signal monitored at point M5 under chirp excitation at point E5.

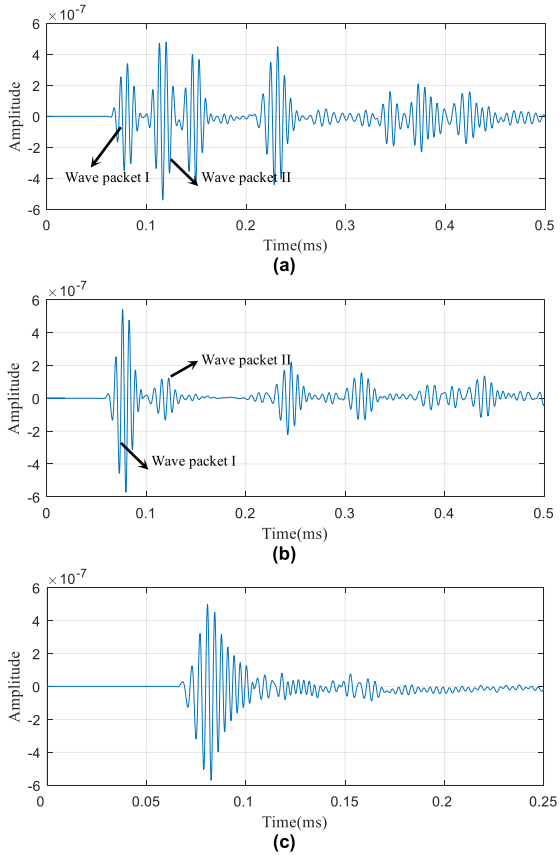

FIGURE 6. Signal extraction results. (a) 100kHz. (b) 200kHz. (c) 300kHz.

of (2) to (5) and the extraction results at 100kHz, 200kHz and 300kHz of tone bust are shown in Fig. 6.

We can clearly see two wave packets from Fig.6(a) and Fig.6 (b), which were assessed firstly by (6) to get the flight time characteristic of signals extracted at different central frequencies. And then the group velocities of the wave packets were calculated by (7), as illustrated in Fig. 7.

Combining dispersion curves shown in Fig. 7 and velocity calculation result (TABLE 2), the first two wave's behavior can be easily characterized for the S0 mode and A0 mode respectively.

Since the propagation velocity of the S0 mode is significantly higher than that of the A0 mode, the S0 mode signal is

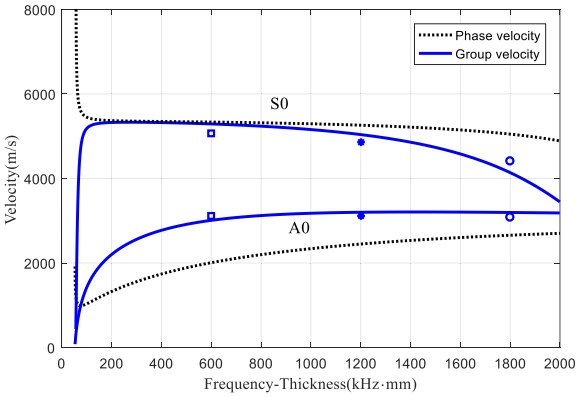

FIGURE 7. Dispersion curves showing phase velocity and group velocity as a function of the multiplication of frequency and thickness. The marked point is the velocity calculation result of the wave packet in the extracted signal at varying central frequencies.

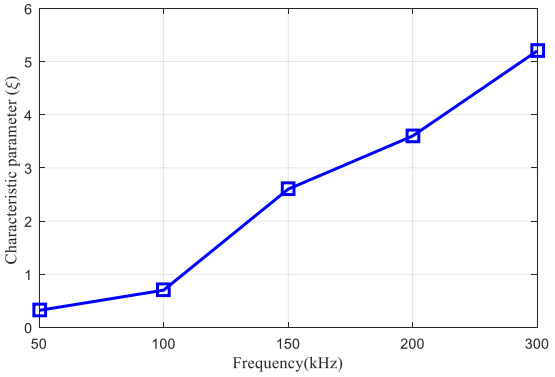

FIGURE 8. Ratio of the S0 mode wave amplitude to A0 mode wave amplitude.

more easily extracted in the signal extraction, and the energy leakage phenomenon of the S0 mode during the propagation process is relatively small so that having longer propagation distance. Therefore, the S0 mode is usually selected as the detection mode in the ultrasonic guided wave nondestructive testing. One of the research focuses of this paper is choosing the central frequency of extraction to obtain pure S0 mode as much as possible. To that end, a new characteristic parameter ξ, defined by the ratio of the S0 mode wave amplitude to the A0 mode wave amplitude, is given.

$$\xi = \frac{A_1}{A_2} \tag{8}$$

where A_1 is the S0 mode wave amplitude and A_2 is the A0 mode wave amplitude. The characteristic parameter ξ at different central frequencies was extracted, as shown in Fig. 8.

As the central frequency of extraction increases, the component of the S0 mode increases, and the component of the A0 mode decreases. Although there is almost pure S0 mode at 300 kHz shown in Fig. 7(c), the dispersion of the S0 mode component appears while the wave packet has obvious tailing phenomenon, so comprehensively consider extracting response signal at the central frequency of 200 kHz.

TABLE 2. Calculation result of the wave packet velocity.

Frequency (kHz)	Theoretical speed of S0 mode (m/s)	Wave packet 1			Theoretical speed of A0 mode (m/s)	Wave packet 2		
		Flight time (ms)	Velocity (m/s)	Relative error (%)		Flight time (ms)	Velocity (m/s)	Relative error (%)
100	5293	0.074	5070	4.2	3006	0.120	3105	3.3
200	5034	0.078	4858	3.5	3200	0.121	3107	2.9
300	4142	0.085	4420	6.7	3196	0.118	3097	3.1

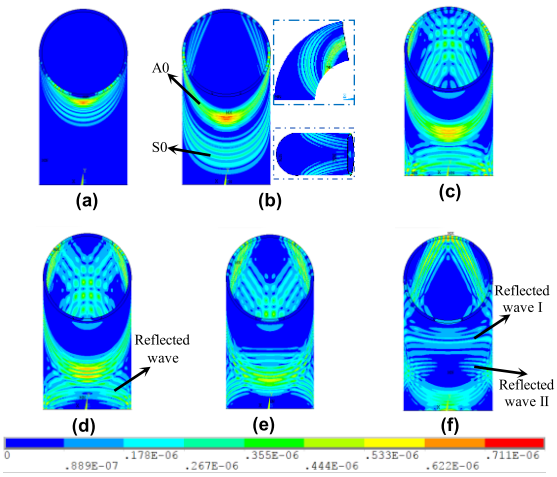

FIGURE 9. Numerical simulation snapshots with E5 point exciting at 100 kHz. (a) 12 μs. (b) 25 μs. (c) 76 μs. (d) 84 μs . (e) 101 μs. (f) 118 μs.

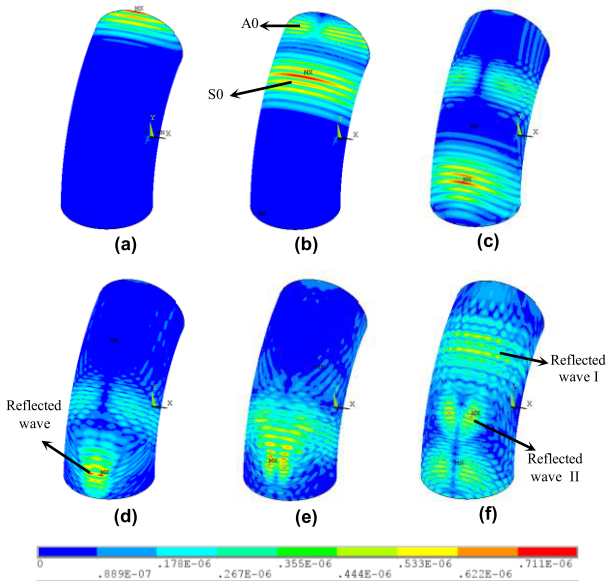

FIGURE 10. Numerical simulation snapshots with E1 point exciting at 200 kHz. (a) 15 μs. (b) 36 μs. (c) 96 μs. (d) 112 μs. (e) 125 μs. (f) 146 μs.

In order to further study the propagation characteristic of the single excitation source guided wave at a specific frequency, the Hanning windowed sinusoid signals centered at 100 kHz and 200 kHz was chosen to generate guided wave at point E5 and point E1 respectively. The wave field snapshots are shown in Fig. 9 and Fig. 10. There are two wave packet and the faster wave is guided wave with S0 mode and the slower wave is guided wave with A0 mode which is in excellent agreement with frontal conclusion. In Fig. 9 (b), the A0 mode has higher energy that is consistent with analysis results of the characteristic parameters at 150 kHz. Through the similar analysis in Fig. 10 (b), we can get the same results that the S0 mode has a higher energy density as the characteristic parameter analyzed at 200 kHz. Moreover, a very interesting phenomenon exists in Fig. 9 and Fig. 10 is that S0 mode will reflect after reaching the end of the elbow, and the reflected signal will interact with the direct A0 mode guided wave generating two wave packets. On the other hand, the energy of the direct A0 mode wave is attenuated, which is why the A0 mode guided wave is usually not used for non–destructive testing.

IV. DEFECT SENSIBILITY OF FLIGHT TIME

It is often thought that the existence of defects can scatter guided wave and present some signatures in the monitored signals [31]. Thus understanding the influence of defects is vital for practical guided wave inspection.

For example, extracting the E1–M1(exciting at E1 point and monitoring at M1 point) signal at 200kHz central frequency to analysis the influence of defects to the propagation guided wave in elbow.

There is an important phenomenon we should pay attention to is that the flight time of S0 mode decreased because of the defect from Fig. 11, which can be explained by the dispersion curve in Fig. 7. The existence of defects will cause the frequency · thickness to decrease whether it is corrosion, cracks or notches; The velocity of the S0 mode in a region with defect will be increased at the central frequency of 200kHz, and the flight time will be lower as a result.

Signals propagating in elbow with defect at different locations were extracted. For example, the physical model was an elbow with defect in intrados. Exciting chirp signal at point E5 and monitoring at positions M(1) to M(8). According to the signal extraction process of (5) to (6), the extracted signals was shown in Fig. 12. Similar analysis was also performed for other excitation points and defects.

Defining η to be flight time variation parameter to quantitatively describe the defect sensitivity.

$$\eta = \frac{t_1 - t_2}{t_1} \times 100\% \tag{9}$$

where t_2 is S0 mode signal flight time in the case of an elbow with defect, t_1 is S0 mode flight time in the case of

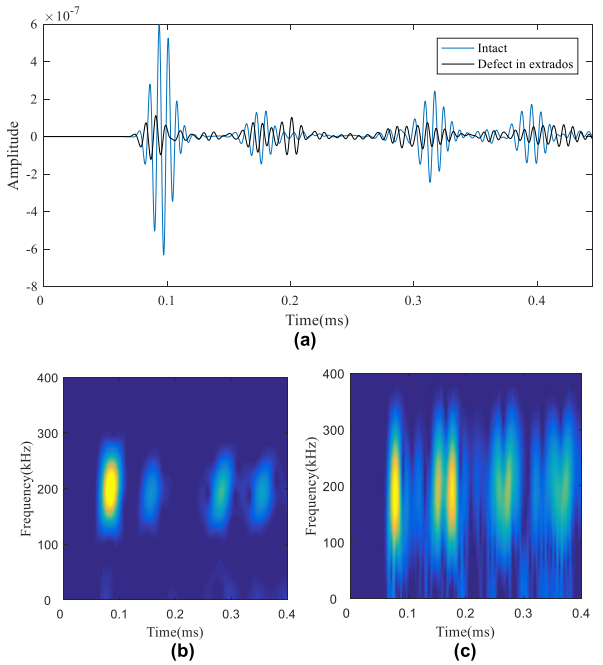

FIGURE 11. Extracted guided wave signals in elbow without defect and with defect in extrados. (a) Time domain waveform signals. (b) Time–frequency domain signal in elbow without defect. (c) Time –frequency domain signal in elbow with defect in extrados.

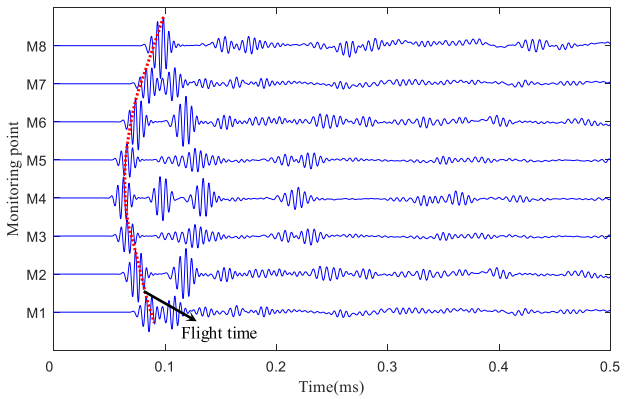

FIGURE 12. Extracted signals at monitoring points (M1 to M8) in elbow with defect in intrados.

an elbow without defect. Elbow model with circumferential crack–like defects in varying position (intrados, extrados and middle of an elbow) were set up. The results of variation parameter under different case of defects are shown in Fig. 13.

From Fig. 13, The value of flight time variation parameters can not only reflect the existence information of defects, but highly dependent on the position of defects. It can be drawn that the flight time variation parameter has good sensibility to the position of defect in elbow. Furthermore, it can be found from Fig. 13 that the variation coefficient of intrados defect is about 2 times larger than that of extrados defect, indicating flight time is more sensitive to defects in intrados.

Fig. 14 shows the received time domain waveform from the traditional excitation method that uses a ring of transducers

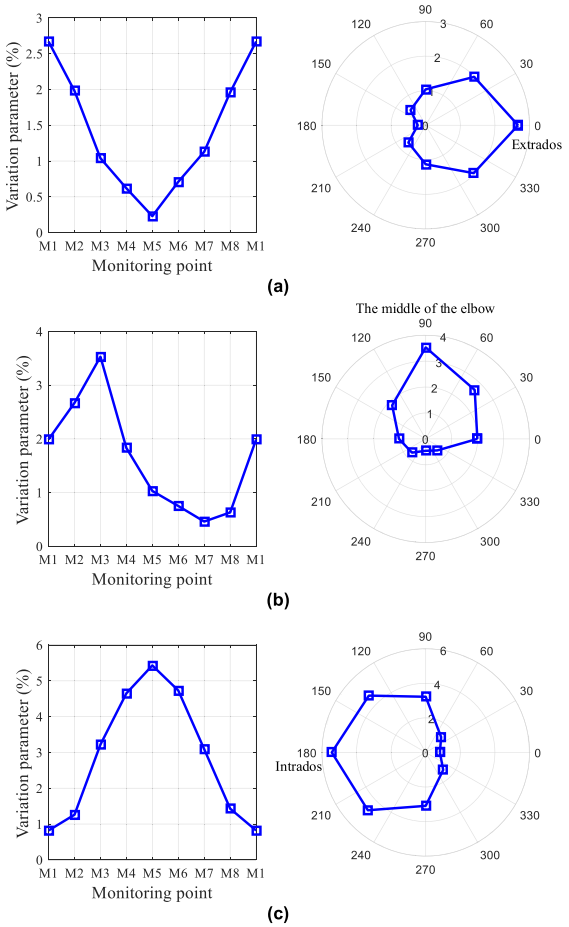

FIGURE 13. Flight time variation parameter with defect in different positions. (a) Defect in extrados. (b) Defect in the middle of the elbow. (c) Defect in intrados.

to generate guided wave at the same time. Figs. 14(a–c) are the waveforms monitored from elbows with defect in intrados, the middle of the elbow and extrados, respectively. It can be found that the waveform reflected by defect is overlap by the waveform reflected by the elbow, especially the defect is in the intrados. Amplitudes of defect reflected waveform in Fig 14. (a) is far less than that in Fig 14. (b) and in Fig 14. (c) which means defect in intrados can be hardly distinguished by the traditional method while our single excitation method proposed has excellent defect sensibility to the defect in intrados. More specifically, the signal obtained by the test usually contains a lot of noise and the flight time features we used are almost immune to noise, while the defect reflected waveform is easily submerged into the noise.

And then relationship between the depth of defect and flight time of S0 mode is studied by changing the depth to 1mm, 2mm, and 3mm. The conclusion is obtained from Fig. 14 that flight time variation parameter becomes larger and larger with the depth of defect increasing. The monitoring point at the direction of defect, such as M1 in Fig. 14(a), M3 in Fig. 14(b) and M5 in Fig. 14(c) is particularly obvious. Thus we can get the conclusion that flight time has good sensibility to the depth of defect in elbow.

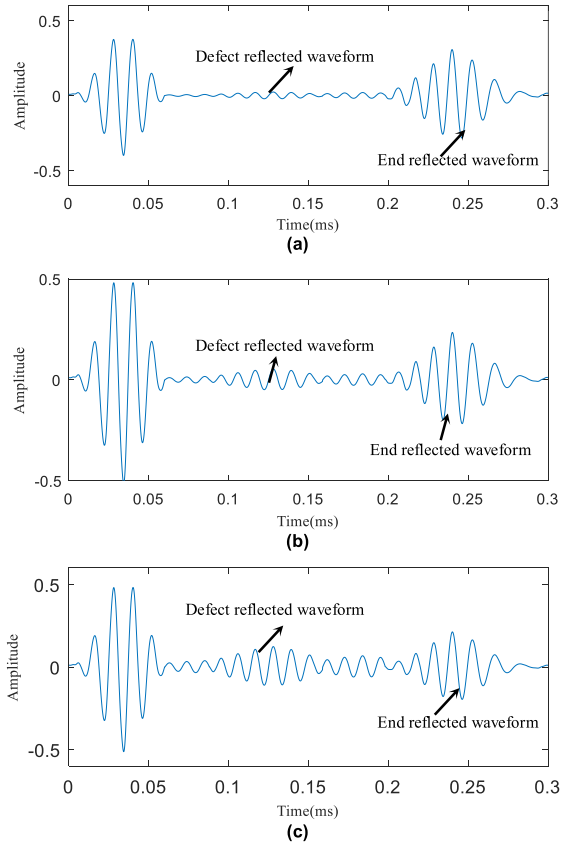

FIGURE 14. Time domain signals generated by a ring of transducers at bends with defect at different locations. (a) Defect in intrados. (b) Defect in the middle of the elbow. (c) Defect in extrados.

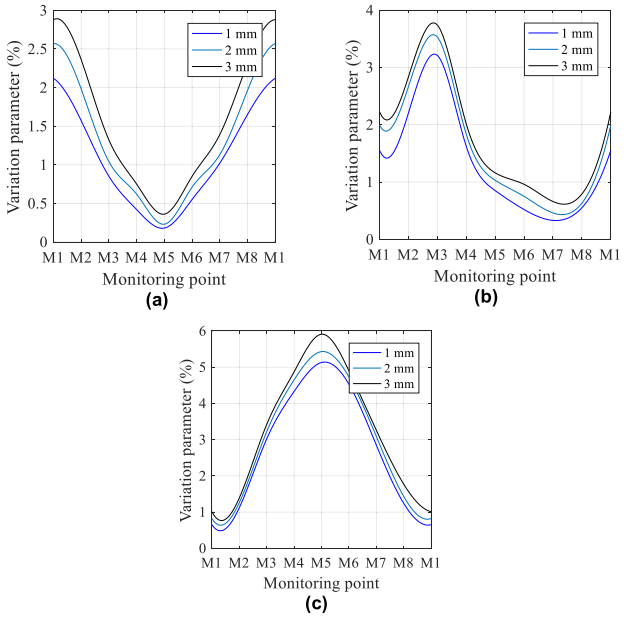

FIGURE 15. Influence of defect depth to flight time variation parameter. (a) Defect in extrados. (b) Defect in the middle of the elbow. (c) Defect in intrados.

V. CONCLUSIONS

This paper studied the propagation characteristics of guided wave from single excitation source in elbow with or without defect via FE method. Using the chirp excitation signal, the transmission signals of guided wave at different excitation central frequencies are extracted with high efficiency. The conclusions are as follows.

(1) Numerical results show that the single excitation source can generate the guided wave including A0 mode and S0 mode. In addition, S0 mode can be generated in the high frequency band as pure as possible. Considering the dispersion and purity, this paper uses central frequency at 200 kHz for signal extraction.

(2) The value of flight time is highly dependent on the position of defects and the flight time variation parameters has good sensibility to defects of elbow. In addition, flight time characteristics is more sensitive to defects in intrados than in other areas, which breaking the limit of being unable to check out the defect in intrados well with the method of a ring of transducers.

(3) With the depth of defect increasing from 1mm to 3mm, flight time variation parameter (η) becomes larger. This finding is significant for the application of guided wave tomography when dealing with quantitative assessment of defects problem.

Under single excitation source, the number of signals monitored can be increased to square of n (n is the number of monitoring points). The data contained in the signal contains large amount of integrity information of the elbow. Further work is needed to establish mappings between flight time and defects to implement data–based non–destructive testing.

REFERENCES

[1] M. H. S. Siqueira, C. E. N. Gatts, R. R. da Silva, and J. M. A. Rebello, "The use of ultrasonic guided waves and wavelets analysis in pipe inspection," *Ultrasonics*, vol. 41, no. 10, pp. 785–797, 2004.
[2] H. Kwun, S. Y. Kim, M. S. Choi, and S. M. Walker, "Torsional guided-wave attenuation in coal-tar-enamel-coated, buried piping," *NDT E Int.*, vol. 37, no. 7, pp. 663–665, Dec. 2004.
[3] D. C. Gazis, "Three-dimensional investigation of the propagation of waves in hollow circular cylinders. I. Analytical foundation," *J. Acoust. Soc. Amer.*, vol. 31, no. 5, pp. 568–573, 1959.
[4] D. C. Gazis, "Errata: Three-dimensional investigation of the propagation of waves in hollow circular cylinders. II," *J. Acoust. Soc. Amer.*, vol. 32, no. 4, pp. 573–578, 1960.
[5] R. Carandente, J. Ma, and P. Cawley, "The scattering of the fundamental torsional mode from axi-symmetric defects with varying depth profile in pipes," *J. Acoust. Soc. Amer.*, vol. 127, no. 6, pp. 3440–3448, 2010.
[6] W. U. Bin, X. Xie, T. W. Peter, L. I. Yuhao, Z. Liu, and H. E. Cunfu, "Numerical simulation on propagation characteristics of low frequency longitudinal guided wave modes in steel floral pipes," *J. Basic Sci. Eng.*, vol. 20, no. 5, pp. 930–939, 2012.
[7] N. Nakamura, H. Ogi, and M. Hirao, "EMAT pipe inspection technique using higher mode torsional guided wave T(0,2)," *NDT E Int.*, vol. 87, pp. 78–84, Apr. 2017.
[8] E. Leinov, M. J. S. Lowe, and P. Cawley, "Investigation of guided wave propagation and attenuation in pipe buried in sand," *J. Sound Vib.*, vol. 347, pp. 96–114, Jul. 2015.
[9] L. Sun, Y. Li, S. Jin, Z. Song, and Y. Zhang, "Study on propagation characteristics of ultrasonic guided waves along the Pipe," in *Proc. 6th World Congr. Intell. Control Automat.*, Jun. 2006, pp. 5177–5181.
[10] R. Murayama and M. Kobayashi, "Pipe inspection system by guide wave using a long distance waveguide," in *Proc. AIP Conf.*, vol. 5, Feb. 2016, pp. 139–149.
[11] W. J. W. J. Z. Xuanshuo, "Ultrasonic guided wave pipeline defect detection using wavelet threshold selection method analysis," *Foreign Electron. Meas. Technol.*, vol. 8, Aug. 2010. pp. 33–40.

[12] R. Murayama, W. Jie, and M. Kobayashi, "Pipe inspection system of a pipe by three-modes guide wave using polarized-transverse wave EMATs," *Proc. SPIE*, vol. 9302, Mar. 2015, Art. no. 93022T.
[13] A. Galvagni and P. Cawley, "A permanently installed guided wave system for pipe monitoring," presented at the Health Monit. Struct. Biol. Syst., 2012. [online]. Available: http://g.wanfangdata.com.cn/details/detail.do?_type=conference&id=CC0212888687
[14] L. Parvizsedghy, A. Senouci, T. Zayed, S. F. Mirahadi, and M. S. El-Abbasy, "Condition-based maintenance decision support system for oil and gas pipelines," *Struct. Infrastruct. Eng.*, vol. 11, no. 10, pp. 1323–1337, 2015.
[15] R. Sanderson, "Inspection of pipe networks containing bends using long range guided waves," presented at the 51st Annu. Conf. Brit. Inst. Non-Destruct. Test., 2012. [online]. Available: http://g.wanfangdata.com.cn/details/detail.do?_type=conference&id=CC0213438924
[16] S. Heinlein, P. Cawley, and T. K. Vogt, "Reflection of torsional T(0,1) guided waves from defects in pipe bends," *NDT E Int.*, vol. 93, pp. 57–63, Jan. 2018.
[17] L. Zhang, P. J. Mudge, J. L. Rose, and M. J. Avioli, "A natural focusing low frequency guided wave experiment for the detection of defects beyond elbows," *J. Pressure Vessel Technol.*, vol. 127, no. 3, pp. 310–316, 2005.
[18] A. Demma, P. Cawley, M. Lowe, and B. Pavlakovic, "The effect of bends on the propagation of guided waves in pipes," *J. Pressure Vessel Technol.*, vol. 127, no. 3, pp. 328–335, 2005.
[19] A. Demma, P. Cawley, M. Lowe, and A. G. Roosenbrand, "The reflection of the fundamental torsional mode from cracks and notches in pipes," *J. Acoust. Soc. Amer.*, vol. 114, no. 2, pp. 611–625, 2003.
[20] R. E. Jones, F. Simonetti, M. J. S. Lowe, and I. P. Bradley, "The effect of bends on the long-range microwave inspection of thermally insulated pipelines for the detection of water," *J. Nondestruct. Eval.*, vol. 31, no. 2, pp. 117–127, 2012.
[21] H. Nishino, S. Masuda, Y. Mizobuchi, T. Asano, and K. Yoshida, "Long-range testing of welded elbow pipe using the T(0,1) mode ultrasonic guided wave," *Jpn. J. Appl. Phys.*, vol. 49, no. 11, Nov. 2010, Art. no. 116602.
[22] H. Nishino, K. Yoshida, H. Cho, and M. Takemoto, "Propagation phenomena of wideband guided waves in a bended pipe," *Ultrasonics*, vol. 44, pp. e1139–e1143, Dec. 2006.
[23] J. J. Tan, W. Xin, N. Guo, and J.-H. Ho, "Computational model considerations of defect detection in pipes with bends using focused guided wave," *J. Chin. Inst. Eng.*, vol. 39, no. 7, pp. 785–793, 2016.
[24] B. Verma, T. K. Mishra, K. Balasubramaniam, and P. Rajagopal, "Interaction of low-frequency axisymmetric ultrasonic guided waves with bends in pipes of arbitrary bend angle and general bend radius," *Ultrasonics*, vol. 54, no. 3, pp. 801–808, 2014.
[25] M. Qi, S. Zhou, N. Jing, and L. Yong, "Investigation on ultrasonic guided waves propagation in elbow pipe," *Int. J. Pressure Vessels Piping*, vols. 139–140, pp. 250–255, Mar./Apr. 2016.
[26] M. J. S. Lowe, V. M. N. Ledesma, E. P. Baruch, and A. Demma, "Guided Wave Testing of an Immersed Gas Pipeline," *Mater. Eval.*, vol. 67, no. 2, pp. 102–115, 2009.
[27] J. L. Rose, D. D. Hongerholt, and D. J. Sames, "Laser based, guided wave experiments for tubing," *Exp. Mech.*, vol. 37, no. 2, pp. 165–168, 1997.
[28] J. E. Michaels, S. J. Lee, A. J. Croxford, and P. D. Wilcox, "Chirp excitation of ultrasonic guided waves," *Ultrasonics*, vol. 53, no. 1, pp. 265–270, 2013.
[29] J. E. Michaels, J. L. Sang, J. S. Hall, and T. E. Michaels, "Multi-mode and multi-frequency guided wave imaging via chirp excitations," *Proc. SPIE*, vol. 7984, pp. 15–24, Mar. 2011.
[30] L. Cohen, "Instantaneous frequency and group delay of a filtered signal," *J. Franklin Inst.*, vol. 337, no. 4, pp. 329–346, 2000.
[31] P. B. Nagy, S. Francesco, and I. Geir, "Corrosion and erosion monitoring in plates and pipes using constant group velocity Lamb wave inspection," *Ultrasonics*, vol. 54, no. 7, pp. 1832–1841, 2014.

YU WANG (S'12–M'15–SM'18) received the B.Eng. degree in mechanical design and manufacturing automation from the Xi'an University of Technology, Xi'an, China, the M.Eng. degree in manufacturing engineering and automation from Xi'an Jiaotong University, and the Ph.D. degree in systems engineering and engineering management from the City University of Hong Kong, Hong Kong. Since 2017, he has been an Associate Professor with the School of Mechanical Engineering, Xi'an Jiaotong University. His current research interests include reliability assessment, fault prognostics, and health management.

XUEYI LI received the B.Eng. degree in mechanical engineering from the Nanjing University of Aeronautics and Astronautics, Nanjing, China. He is currently pursuing the M.Eng. degree in mechanical engineering with the School of Mechanical Engineering, Xi'an Jiaotong University.